Journal of Nuclear Materials 400 (2010) 32–36

Contents lists available at ScienceDirect

Journal of Nuclear Materials

journal homepage: www.elsevier.com/locate/jnucmat

Melting behavior of MgO-based inert matrix fuels containing $(Pu,Am)O_{2-x}$

Shuhei Miwa *, Isamu Sato, Kosuke Tanaka, Takashi Hirosawa, Masahiko Osaka

Oarai Research and Development Center, Japan Atomic Energy Agency, 4002 Narita-cho, Oarai-machi, Higashi-ibaraki-gun, Ibaraki 311-1393, Japan

ARTICLE INFO

Article history:
Received 1 October 2009
Accepted 5 February 2010

ABSTRACT

The melting behavior of MgO-based inert matrix fuels containing $(Pu,Am)O_{2-x}$ ($(Pu,Am)O_{2-x}$–MgO fuels) was experimentally investigated. Heat-treatment tests were carried out at 2173 K, 2373 K and 2573 K each. The fuel melted at about 2573 K in the eutectic reaction of the Pu–Am–Mg–O system. The $(Pu,Am)O_{2-x}$ grains, MgO grains and pores grew with increasing temperature. In addition, Am-rich oxide phases were formed in the $(Pu,Am)O_{2-x}$ phase by heat-treatment at high temperatures. The melting behavior was compared with behaviors of PuO_{2-x}–MgO and AmO_{2-x}–MgO fuels.

1. Introduction

Inert matrix fuels (IMFs) with a high content of minor actinides (MAs) are considered as one promising option for the rapid incineration of MAs in a future fast reactor fuel cycle system and an accelerator-driven sub-critical system [1–5]. IMFs are a composite of MA host phase and an inert matrix (IM). Magnesium oxide (MgO) is considered to be a promising candidate for an IM [1–5]. MgO was selected based on an evaluation of its high manufacturability, chemical/physical stability, high melting temperature, and relatively high thermal conductivity. Namely, these good thermal properties can lead to a low operating temperature and large safety margin in the case of accidental melting of fuel. Plutonium and americium mixed oxide ($(Pu,Am)O_{2-x}$) is considered to be a candidate of a MA oxide host phase for the MgO IM [1–5]. The development of a fabrication technology and characterization of MgO-based IMFs containing $(Pu,Am)O_{2-x}$ ($(Pu,Am)O_{2-x}$–MgO fuels) are now underway [1,2,6–9]. Table 1 summarizes the fundamental specifications of the $(Pu,Am)O_{2-x}$–MgO fuels which have been investigated.

The maximum temperature of the fuels during irradiation and severe accidents is limited within the design criterion to prevent fuel melting. The melting temperatures of MgO, PuO_2 and AmO_2 are 3250 K [10], 2843 K [11] and 2773 K [11], respectively. It was, however, found that the liquid phase started to form in the respective Pu–Mg–O and Am–Mg–O systems at 2503 K [12] and 2350 K [13] in an eutectic reaction. These temperatures were clearly lower than the respective melting temperatures of MgO, PuO_2 and AmO_2. In addition, the eutectic temperatures depended on oxygen deficiencies of PuO_{2-x} and AmO_{2-x}. The eutectic temperature of Pu–Mg–O system was estimated by a calculation and found to decrease with decreasing oxygen to metal (O/M) ratio from about 2503 K for O/M ratio of 2.00 to 2341 K for O/M ratio of 1.61 [12]. On the other hand, the eutectic temperature of Am–Mg–O system was also estimated by a calculation and had the maximal value of 2350 K for O/M ratio of 1.79 and the very low temperature of 1930 K for O/M ratio of 1.5 [13]. Since the oxygen potential of Am-containing oxides has been found to be very high [14–16], Am-containing oxides in MgO-based IMF could be easily reduced at high temperature. This could lead to lowering of eutectic temperature of MgO-based IMFs. Therefore for the fuel design, it is important to investigate the melting behavior of MgO-based IMFs with Am-containing oxide.

However, experimental data for the melting behavior of MgO-based IMFs are limited, and there are no data for the melting behavior of $(Pu,Am)O_{2-x}$–MgO fuels. In this study, therefore, the melting behavior of $(Pu,Am)O_{2-x}$–MgO fuels was experimentally investigated. Heat-treatments at various temperatures were carried out, and the melting behavior of $(Pu,Am)O_{2-x}$–MgO fuels was compared with behaviors of PuO_{2-x}–MgO and AmO_{2-x}–MgO fuels.

2. Experimental

The micro-dispersed type $(Pu,Am)O_{2-x}$–MgO fuels (host phase size below 10 μm in diameter) were prepared for the heat-treatment tests. The micro-dispersed type fuels were considered as conventional type fuels because it could be fabricated by using simple powder metallurgy, which was adaptable to remote operation [7–9]. The fabrication procedure consisted of the following steps: heat-treatment of $(Pu,Am)O_2$ powder at 903 K; milling of the $(Pu,Am)O_2$ powder in a ball mill for 3 h using Al_2O_3 balls; weighing each powder to get the composition of 50 wt.% $(Pu,Am)O_2$ and 50 wt.% MgO; mixing of these powders for 5 min; cold pressing of the final mixed powder at 400 MPa into a compact; sintering

---

* Corresponding author. Tel.: +81 29 267 4141; fax: +81 29 266 0016.
E-mail address: miwa.shuhei@jaea.go.jp (S. Miwa).

0022-3115/$ - see front matter © 2010 Elsevier B.V. All rights reserved.
doi:10.1016/j.jnucmat.2010.02.006

Table 1
Fundamental specifications of the $(Pu,Am)O_{2-x}$–MgO fuels.

Fuel	Shape density	Sintered columnar pellet 90% TD
Host phase	Chemical form	$(Pu,Am)O_{2-x}$
	Weight fraction	0.50
	Morphologic shape	Particle <10 μm in diameter
Inert matrix phase	Chemical form	MgO

the compact at 1873 K in air atmosphere. Table 2 summarizes the characteristics of micro-dispersed type $(Pu,Am)O_{2-x}$–MgO fuels [9].

These fuels were heat-treated in a high-frequency induction heating furnace in flowing Ar gas. The pellet specimens were loaded into a molybdenum (Mo) crucible. The temperature at the bottom of the crucible was monitored by a pyrometer under the furnace, and was regarded as the specimen temperature. The pyrometer was calibrated by observing the melting temperatures of niobium (2742 K [17]) and vanadium (2108 K [18]). Oxygen partial pressure in flowing Ar gas was adjusted as 10^{-6} atm by dilution of O_2. The heat-treatment temperatures were 2173 K, 2373 K and 2573 K each. The heating rate was 180 K/min above 1273 K and the holding time was 1 h. After holding, the specimens were naturally cooled, and the resultant cooling rate was about 100 K/min. The heat-treatment at 2573 K was stopped in 10 min because there was indication of melting.

The $(Pu,Am)O_{2-x}$–MgO fuels heat-treated at high temperatures were characterized in terms of their microstructures, crystal structures and element distributions.

The microstructure was observed with an optical microscope (TELATOM, Reichert). The $(Pu,Am)O_{2-x}$–MgO fuels heat-treated were mounted into holders using epoxy resin, and then were ground and mirror-polished with anhydrous lubricant.

Crystal structures were observed by XRD analysis. The O/M ratio of $(Pu,Am)O_{2-x}$ phase was calculated from the lattice parameter by using Vegard's law, in which $(Pu,Am)O_{2-x}$ was assumed as an ideal solid solution of PuO_2, $PuO_{1.62}$, AmO_2 and $AmO_{1.61}$ [9].

The element distributions of Pu, Am and Mg was investigated by using an electron probe micro-analyzer (EPMA) (SX-100R, AMETEK). Electron acceleration energy of 25 kV and a beam current of 50 nA were selected for the analysis. Selected characteristic X-rays were Mα lines for Pu and Am, and the Kα line for Mg. Qualitative image mapping of X-ray intensities and quantitative point analysis were conducted on polished specimens which were coated with deposited carbon. Calibration data of Pu, Am and Mg were obtained using an as-fabricated $(Pu,Am)O_{2-x}$–MgO fuel and the raw X-ray data were converted to a weight fraction using the Cameca matrix correction program based on the PAP model [19].

3. Results and discussion

Fig. 1 shows the visual aspects of $(Pu,Am)O_{2-x}$–MgO fuels heat-treated at 2373 K and 2573 K. Whereas the pellet heat-treated at 2373 K maintained its integrity, the pellet heat-treated at 2573 K showed partial melting in its shape. Fig. 2 reproduces the ceramographic images of $(Pu,Am)O_{2-x}$–MgO fuels heat-treated at 2173 K, 2373 K and 2573 K each, and also an image from an as-fabricated one. The light gray-colored areas and the dark gray-colored areas show the $(Pu,Am)O_{2-x}$ phase and the MgO phase, respectively. $(Pu,Am)O_{2-x}$ grains, MgO grains and pores grew with increasing temperature. No indication of liquid phase formation was observed in the $(Pu,Am)O_{2-x}$–MgO fuels heat-treated at 2173 K and 2373 K. It should be noted that MgO grains for the 2573 K heat-treatment had island shapes. This structure indicated the coexistence of MgO solid phase and liquid phase at this elevated temperature. This result indicated that the eutectic reaction of the Pu–Am–Mg–O system occurred at 2573 K.

Table 2
Characteristics of $(Pu,Am)O_{2-x}$–MgO fuels [9].

Composition of host phase	$(Pu_{0.91}Am_{0.09})O_{2-x}$
Weight fraction	0.50
Density	$5.14\ g/cm^3$ (93.5% TD)
Lattice parameter	0.5398 nm

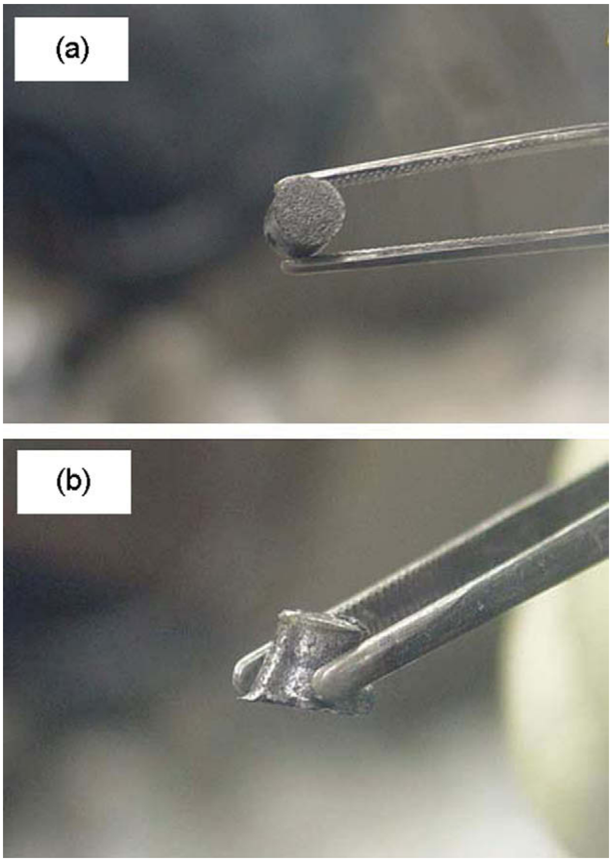

Fig. 1. Visual aspects of $(Pu,Am)O_{2-x}$–MgO fuels, (a) 2373 K and (b) 2573 K.

Fig. 3 shows the XRD patterns of $(Pu,Am)O_{2-x}$–MgO fuels heat-treated at 2173 K, 2373 K and 2573 K each. The results for an as-fabricated $(Pu,Am)O_{2-x}$–MgO fuel are also given. There were only peaks derived from the halite structure for MgO and the fluorite structure for $(Pu,Am)O_{2-x}$. No reaction phase with MgO and $(Pu,Am)O_{2-x}$ was observed. Although the formation of precipitate phases was observed by EPMA results as described below, no peaks of a precipitate phase were detected due to its low volume in $(Pu,Am)O_{2-x}$ phases. Table 3 lists the lattice parameters and calculated O/M ratios of $(Pu,Am)O_{2-x}$. The O/M ratios of $(Pu,Am)O_{2-x}$ were decreased by the heat-treatment.

The variations of eutectic temperature with oxygen deficiency of Pu–Mg–O and Am–Mg–O systems were represented by two regression equations [12,13]:

$$T_{m.Pu} = -688 + 3053(O/Pu) - 729(O/Pu)^2 \quad \text{for} \quad 1.61 \leqslant (O/Pu) \leqslant 2, \tag{1}$$

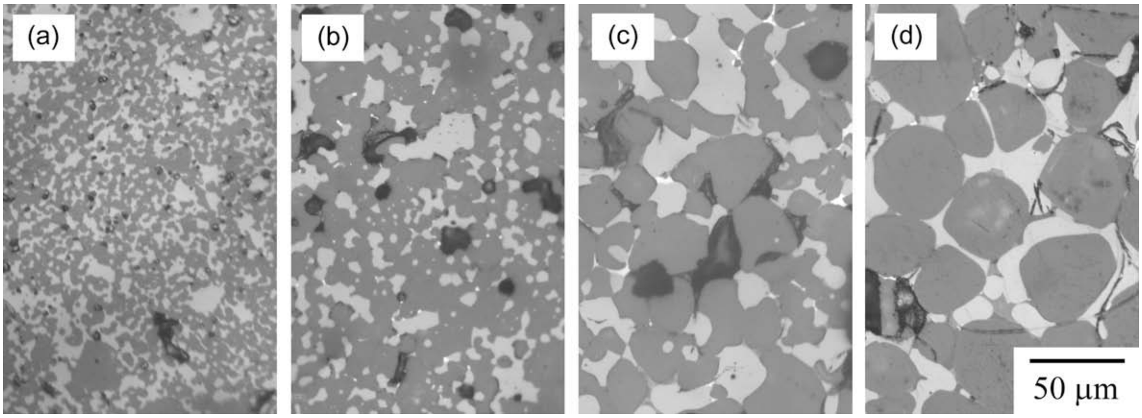

Fig. 2. Ceramographic images of (Pu,Am)O_{2-x}–MgO fuels, (a) as-fabricated and with heat-treatments at (b) 2173 K, (c) 2373 K, and (d) 2573 K each.

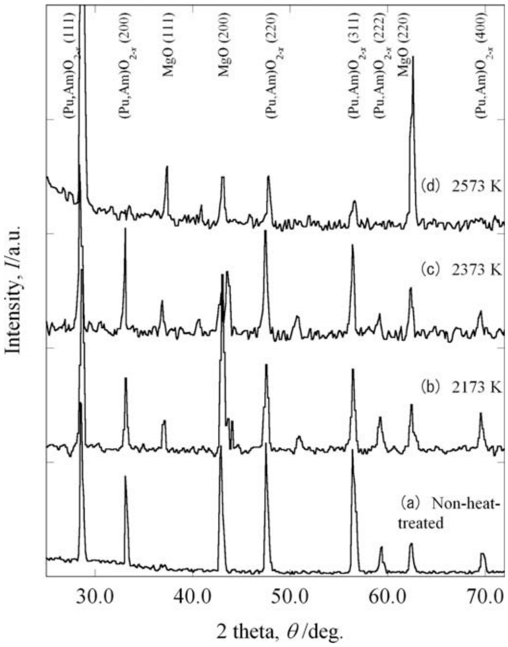

Fig. 3. XRD patterns of (Pu,Am)O_{2-x}–MgO fuels, (a) as-fabricated and with heat-treatments at (b) 2173 K, (c) 2373 K, and (d) 2573 K each.

Table 3
Lattice parameters and calculated O/M ratios of (Pu,Am)O_{2-x}.

Heat-treatment temperature (K)	Lattice parameter (nm)	O/M ratio[a]
As-fabricated	0.5398[b]	1.99[b]
2173	0.5418	1.93
2373	0.5415	1.94
2573	0.5406	1.97

[a] Calculated by Vegard's law.
[b] Ref. [9].

$$T_{m.Am} = 2221(1-N) + 2291N + N(1-N)\ [236.6 + 1578.6N - 3478.0N^2 + 1908.8N^3],$$

$$N = [(O/Am) - 1.62]/0.38 \quad for \quad 1.62 \leqslant (O/Am) \leqslant 2, \qquad (2)$$

where $T_{m.Pu}$ and $T_{m.Am}$ are eutectic temperatures of Pu–Mg–O and Am–Mg–O systems, respectively. The eutectic temperatures of Pu–Mg–O and Am–Mg–O systems at the calculated O/M ratio in this study are shown in Table 4. The eutectic temperatures of Pu–Mg–O system were all higher than those of Am–Mg–O system. The heat-treatment temperature of 2573 K was higher than the eutectic temperatures of both Pu–Mg–O and Am–Mg–O systems. Therefore, the melting of the (Pu,Am)O_{2-x}–MgO fuel at 2573 K was attributed to the eutectic reaction as mentioned above. On the other hand, although the heat-treatment temperature of 2373 K was higher than the eutectic temperature of the Am–Mg–O system, there was no indication of liquid phase formation from the results of microstructure observation. This result showed that the eutectic temperature of Pu–Am–Mg–O system would be higher than that of Am–Mg–O system. Although the effects of the interaction between Pu and Am on melting behavior of (Pu,Am)O_{2-x}–MgO fuel should be investigated in further experiments, the present results have shown the possibility to increase the eutectic temperature of Am–Mg–O system by Pu dissolving into AmO_{2-x}.

Fig. 4 shows the secondary electron images and qualitative characteristic X-ray mappings of Pu, Am and Mg in (Pu,Am)O_{2-x}–MgO fuels heat-treated at 2173 K, 2373 K and 2573 K each. The results for an as-fabricated one are also given. Since the (Pu,Am)O_{2-x} and MgO phases were fine in the as-fabricated (Pu,Am)O_{2-x}–MgO fuel and their size was below the measurable limit of EPMA (about 2–3 μm), mixed distributions of Pu, Am and Mg were observed (blue[1] colored region in Fig. 4a). Regarding the heat-treated (Pu,Am)O_{2-x}–MgO fuels, the intensity of the characteristic X-ray peaks of Am in (Pu,Am)O_{2-x} slightly decreased with increasing temperature. Conversely, that of Pu in (Pu,Am)O_{2-x} increased with increasing temperature. Fig. 5 shows details of the radial distribution of Am metal concentration in (Pu,Am)O_{2-x} phase (Am/(Am + Pu)). The error bars denote plus or minus one standard deviation calculated from 4 to 6 data points. The concentration of Am decreased at the pellet periphery for the heat-treatment at 2173 K. It gradually decreased from the middle to the pellet periphery for the heat-treatment at 2373 K. Regarding the (Pu,Am)O_{2-x}–MgO fuel heat-treated at 2573 K, the concentration of Am became lower than that of 2173 K and 2373 K, and had a homogeneous distribution. These redistribution behaviors of Am indicated that the Am or Am oxides were selectively vaporized from the pellet surface at the heat-treatment conditions. The vaporization pressure of Am and Am oxides has been found to be very high; the vapor pressure of gaseous Am oxide was higher than that of gaseous Pu oxide, in particular that of Am monoxide was about ten times higher than that of Pu monoxide [20]. Therefore,

---

[1] For interpretation of the references to color in this figure, the reader is referred to the web version of this article.

Table 4
The eutectic temperatures of Pu–Mg–O [12] and Am–Mg–O [13] systems at calculated O/M ratio.

O/M ratio	Heat-treatment temperature (K)	Eutectic temperature (K)	
		Pu–Mg–O [12]	Am–Mg–O [13]
1.933	2173	2490	2314
1.940	2373	2491	2312
1.967	2573	2497	2303

the concentration of Am at the pellet periphery would decrease at high temperature, and Am would diffuse on the concentration gradient toward the pellet periphery. This behavior would be enhanced with increasing temperature. For (Pu,Am)O_{2-x}–MgO fuel heat-treated at 2573 K, since each (Pu,Am)O_{2-x} phase area became liquid and was connected as shown in Fig. 2d, the diffusion of Pu and Am would be enhanced through the connected (Pu,Am)O_{2-x} liquid phase areas. This would lead to the homogeneous distribution of Pu and Am.

In addition, it should be noted that Am-rich (Pu,Am)O_{2-x} phases were observed in the heat-treated (Pu,Am)O_{2-x}–MgO fuels as shown in Fig. 4 (white colored regions). These precipitate phases were formed in the vicinity of the interface between the (Pu,Am)O_{2-x} phase and the MgO phase. The size and the number density of these precipitate phases increased with increasing temperature. The Am concentration in these phases was very high, and reached about 90 wt.%. The structure of these phases was considered to be a sesqui-oxide since the phases would have low metal density. It was confirmed by the results that the total intensities of the characteristic X-ray peaks of these precipitate phases were somewhat low (about 80%) compared with the other phases. Am-containing oxides were found to have high oxygen potential [14–16] and, therefore, the formation of sesqui-oxide in Am-rich phases would be reasonable in the heat-treatment conditions.

The data of phase relations of (Pu,Am)O_{2-x} are limited, and such a phase separation has not been reported. Regarding the phase relation of PuO_{2-x} and AmO_{2-x}, it was found that the phase diagram for the Am–O system was similar to that of the Pu–O system, although phase transition temperatures from the single phase to two phases of the Am–O system near stoichiometry were higher than those corresponding to the Pu–O system [21]. Meanwhile, the phase relation of $(Pu_{0.91}Am_{0.09})O_{2-x}$ seemed to have different trends on reaching a certain O/M ratio [22]. This behavior could be well interpreted by the hypothesis that Am was preferentially

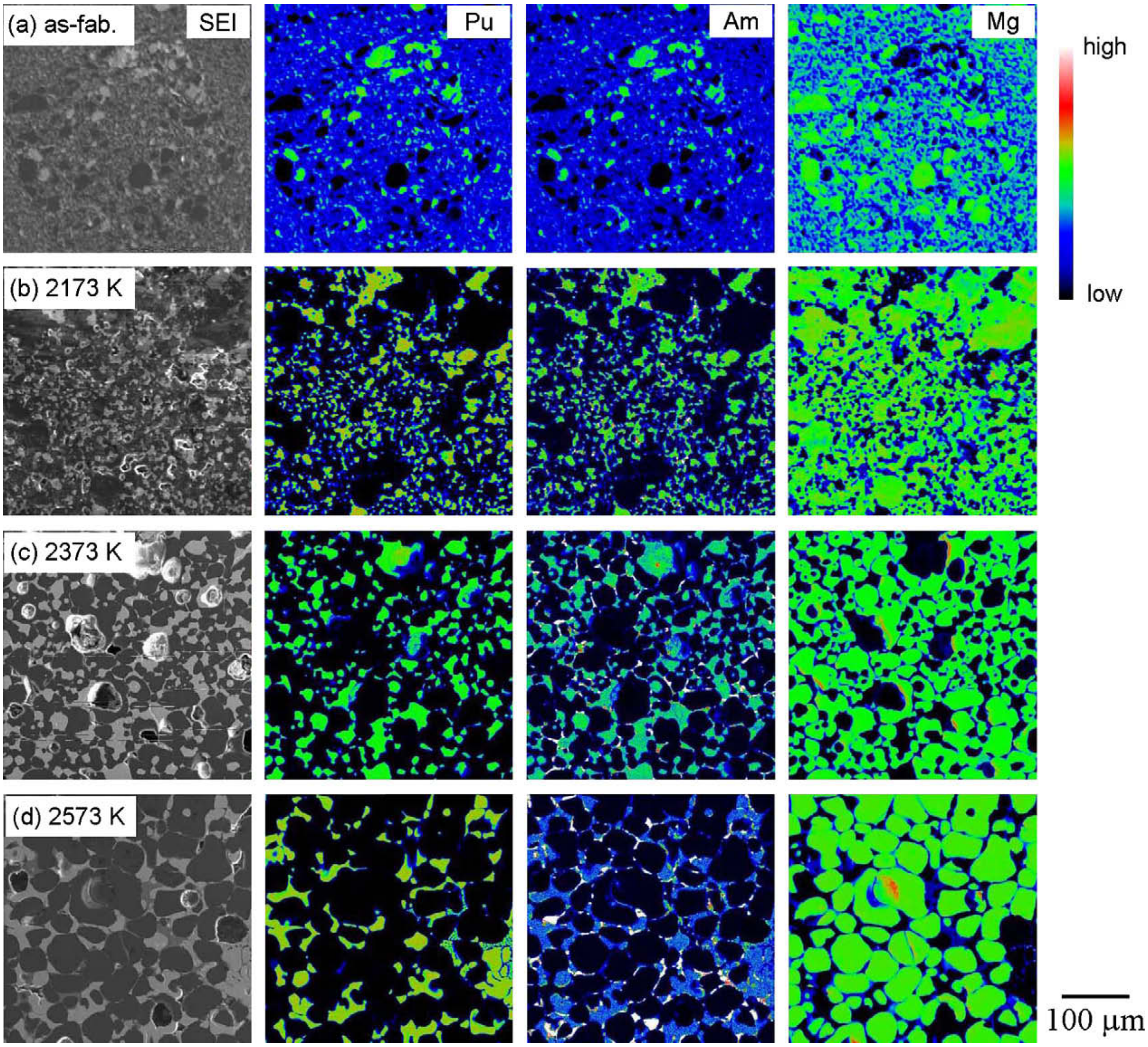

Fig. 4. Distributions of Pu, Am and Mg in (Pu,Am)O_{2-x}–MgO fuels, (a) as-fabricated and with heat-treatments at (b) 2173 K, (c) 2373 K, and (d) 2573 K each.

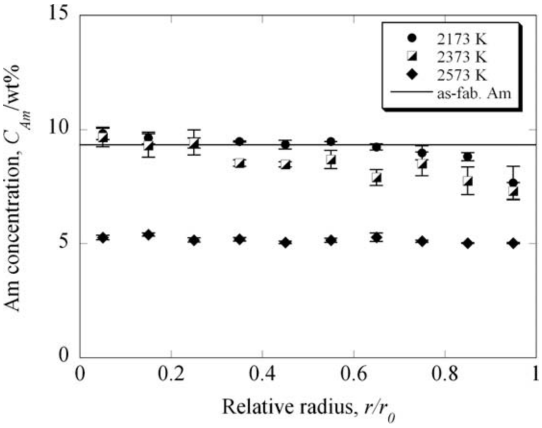

Fig. 5. The detailed distribution of Am metal concentration in (Pu,Am)O_{2-x} phase (Am/(Am + Pu)) heat-treated at 2173 K, 2373 K and 2573 K each.

reduced. This behavior was also confirmed in terms of oxygen potential of (Pu,Am)O_{2-x} [15,16]. These results indicated that tetravalent Am would be instable in (Pu,Am)O_{2-x}. From them, it could be said that the phase separation to the Am-rich sesqui-oxide phase, in which Am was trivalent, would be energetically more favorable rather than the single phase of (Pu,Am)O_{2-x} at high temperature.

These instabilities of Am in (Pu,Am)O_{2-x}, in particular the redistribution of Am and phase separation, can become a critical issue for the design of (Pu,Am)O_{2-x}–MgO fuels, because a possible resultant agglomeration of Am in a specific region of the fuels causes unfavorable property changes such as decrease of melting temperature both by direct effect of increased Am content and derived effect via phase changes. Although no effect of Am-rich phases on melting behavior could be observed in the (Pu,Am)O_{2-x}–MgO fuels in which Am content was only 9%, consideration should be given if the high Am-containing (Pu,Am)O_{2-x} phase would be applied for the host phase of IMFs.

4. Concluding remarks

The melting behavior of the MgO-based IMFs containing (Pu,Am)O_{2-x} was experimentally investigated. The heat-treatment tests at 2173 K, 2373 K and 2573 K each were carried out.

Although (Pu,Am)O_{2-x}–MgO fuels maintained their shape integrity at 2173 K and 2373 K, the fuel melted at 2573 K due to a eutectic reaction, and this temperature was almost the same as the eutectic temperature of the Pu–Mg–O system. The microstructure of fuels changed by heat-treatment; MgO grains, (Pu,Am)O_{2-x} grains and pores grew with increasing temperature. In addition, Am-rich oxide phases, which would be sesqui-oxides, were formed, and the size and number density of Am-rich oxide phases increased. At 2373 K, which was higher than the eutectic temperature of the Am–Mg–O system, there was no indication of melting although there were Am-rich oxide phases.

Detailed effects of the interaction between Pu and Am on melting behavior of (Pu,Am)O_{2-x}–MgO fuel should be investigated through further experiments. Nevertheless, it is believed that the melting temperature of MgO-based IMFs with Am-containing oxide would increase by Pu dissolving into AmO_{2-x}.

Acknowledgements

The authors wish to thank Mr. Kenya Tanaka, Mr. Shoji Onose and Mr. Hiroshi Yoshimochi of JAEA, Mr. Shinichi Sekine and Mr. Takashi Ishida of the Nuclear Technology and Engineering Corporation and Mr. Takayuki Seki and Mr. Naoki Kashimura of the Inspection Development Corporation for their invaluable help in these experiments.

References

[1] M. Osaka, H. Serizawa, M. Kato, K. Nakajima, Y. Tachi, R. Kitamura, S. Miwa, T. Iwai, K. Tanaka, M. Inoue, Y. Arai, J. Nucl. Sci. Technol. 44 (2007) 309.
[2] M. Osaka, S. Miwa, K. Tanaka, I. Sato, T. Hirosawa, H. Obayashi, K. Mondo, Y. Akutsu, Y. Ishi, S. Koyama, H. Yoshimochi, K. Tanaka, in: C.A. Brebbia, V. Popov (Eds.), Energy and Sustainability, Transaction: Ecology and the Environment, vol. 105, Wessex Institute of Technology, UK, 2007, p. 357.
[3] Y. Croixmarie, E. Abonneau, A. Fernandez, R.J.M. Konings, F. Desmouliere, L. Donnet, J. Nucl. Mater. 320 (2003) 11.
[4] W. Maschek, X. Chen, F. Delage, A. Fernandez-Carretero, D. Haas, Prog. Nucl. Energy 50 (2–6) (2008) 333.
[5] F. Jorison, C. Maillard, J.C. Martin, L. Donnet, N. Drin, in: Proceedings of GLOBAL 2007, Boise, ID, USA, September 9–13, 2007, pp. 1353.
[6] S. Miwa, M. Osaka, K. Tanaka, Y. Ishi, H. Yoshimochi, K. Tanaka, in: Proceedings of GLOBAL 2007, Boise, ID, USA, September 9–13, 2007, pp. 903.
[7] M. Osaka, S. Miwa, Y. Tachi, Ceram. Int. 32 (2006) 659.
[8] S. Miwa, M. Osaka, J. Nucl. Mater. 385 (2009) 165.
[9] S. Miwa, Y. Ishi, M. Osaka, J. Nucl. Mater. 389 (2009) 402.
[10] C. Ronchi, M. Sheindlin, J. Appl. Phys. 90 (2001) 3325.
[11] M. Kato, K. Morimoto, H. Sugata, K. Konashi, M. Kashimura, T. Abe, J. Nucl. Mater. 373 (2008) 237.
[12] H. Zhang, M.E. Huntelaar, R.J.M. Konings, E.H.P. Cordfunke, J. Nucl. Mater. 249 (1997) 223.
[13] H. Zhang, M.R.J.M. Konings, E. Huntelaar, E.H.P. Cordfunke, J. Nucl. Mater. 250 (1997) 88.
[14] T.D. Chikalla, L. Eyring, J. Inorg. Nucl. Chem. 29 (1967) 2281.
[15] H. Otobe, M. Akabori, Y. Arai, J. Nucl. Mater. 389 (2009) 68.
[16] M. Osaka, K. Kurosaki, S. Yamanaka, J. Nucl. Mater. 357 (2006) 69.
[17] R.E. Bedford, G. Bonnier, H. Maas, F. Pavese, Metrologia 33 (1996) 133.
[18] M.W. Chase (Ed.), Journal of Physical and Chemical Reference Data, Monograph 9, American Chemical Society, American Institute of Physics, NY, USA; 1998, pp. 1918.
[19] J.L. Pouchou, F. Pichoir, La Rech. Aérospatiale 3 (1984) 13.
[20] R.J. Ackermann, R.L. Faircloth, M.H. Rand, J. Chem. Phy. 70 (1966) 3698.
[21] C. Sari, E. Zamorani, J. Nucl. Mater. 37 (1970) 324.
[22] S. Miwa, M. Osaka, H. Yoshimochi, K. Tanaka, K. Kurosaki, M. Uno, S. Yamanaka, J. Alloys Compd. 444–445 (2007) 610.